Probe diagnostics in high pressure high density microwave plasma

Mamunur Rashid Talukder*, Dariusz Korzec** and Masashi Kando**

Abstract

High pressure helium microwave discharge by the moderate microwave power of 400W has been investigated. A method for the determination of electron temperature and the plasma density by a Langmuir probe is established using Cohen model in the asymptotic limits of $D_\lambda = R_p/\lambda_D \to \infty$, $\varepsilon = T_+/T_e \to 0$ and $0 \le \varphi_p \le \ln(D_\lambda)$, where R_p, λ_D, D_λ, T_+, T_e and φ_p are the probe radius, the electron Debye length, the Debye number, ion and electron temperatures and the probe potential normalized by electron energy, respectively. Simple algebraic functions derived from Cohen's results allow one to use iterative procedures for the determination of plasma parameters and avoid making the fitting parameters discrete. The proposed fitting technique allows one to obtain reasonable plasma parameters even for high secondary electron emission currents from the probe.

1.Introduction

High pressure discharges are of increasing interest for the reactive plasma processing[1]. There are several convenient features of the microwave excited high pressure non-thermal plasmas. In such plasmas, gas flow rate can be much lower, power transfer from a generator to plasma becomes higher, gas temperature becomes much lower and the electrode contamination is devoid. Additional features are the stability and feasible operation. Microwave discharge can be operated over a wide range of experimental parameters (pressure: from 10^{-5} Torr up to atmospheric pressure, microwave power: from several watts up to kilowatts, frequency: from 10MHz up to 10GHz), which facilitate to control the plasma in a variety of parameters[2].

High pressure plasma processing can provide several advantages over low pressure plasma one. There is no need of the equipment for magnetic field generation and high vacuum systems, which can largely reduce the equipment cost. Furthermore, high pressure plasmas enable one to produce large amount of reactive species like ions, excited atoms and free radicals. Therefore, high pressure discharges have been used for gas discharge lasers or the ozone production for water purification[3].

For plasma source design and discharge performance optimization, good knowledge of plasma parameters and their spatial distributions are required. In order to interpret the data measured under different experimental conditions[4], it is important to have a proper theoretical model, which can provide reliable plasma parameters. The Langmuir probe is a most widely used diagnostic tool for the determination of plasma parameters because it can provide local plasma properties that cannot be obtained by other diagnostic techniques. The pioneer model of the probe diagnostic has been developed for the low pressure plasmas by Langmuir and Mott-Smith[5], where the collisions of charged particles with neutral particles within the sheath region can be neglected. Their results are strictly valid only for the cases where the sheath thickness or the electron Debye length is much larger than the probe dimension. With increasing pressure, the mean free paths of electrons and ions become much shorter than the probe dimension so that their collisions have strong influence on probe measurements. There are several theoretical kinetic models* of the collisional plasmas[6-10] for the probe diagnostics. Waymouth[6] assumed $\lambda_e/R_p < 10$, $R_p/100\,\lambda_D > 1$, $\lambda_e/\lambda_D > 10$ where R_p, λ_e and λ_D are the probe radius, the electron mean free path and the electron Debye length, respectively. He assumed also that the plasmas are diffusion-controlled and that the electrons have Maxwellian energy distribution. Waymouth showed that the results obtained under the assumed conditions reduce to the results by Langmuir and Mott-Smith[5] as the mean free paths become long. Bienkowski and Chang[7] considered a small Debye length but an arbitrary ion mean free path for highly negative probe potentials. They presented current-voltage probe characteristics in a form useful for the direct prediction of the electron density, provided the electron mean free path is known. Zakrzewski and Kopiczynski[9] considered the condition that the Debye number $D_\lambda = R_p/\lambda_D$ is smaller than 3 and that there are very few collisions in the sheath region. They provided physical arguments for the effects of the charged particle collisions on their currents to the probe. One of the effects is due to the collision of charged particles with the neutral particles within the space charge sheath, which causes an increase of charged particle currents to the probe due to the destruction of the orbital motion of the charged particles. In this case, the charged particles will lose their energies due to the collisions with the neutral particles within the sheath region so that they will be trapped in the potential well near the probe surface and consequently will be collected by the probe. This phenomenon dominates at a pressure higher than 1 Torr. The other effect is a decrease in the charged particle currents to the probe[10, 11]. In this case, the charged particles will be scattered through the collisions in the sheath and can escape from the potential well. As a result, the probe current decreases. However, when the charged particles will not be able to escape from the potential well, the probe will collect them. The amount of the probe current may depend on the direction and angle of

* Graduate School of Electronic Science and Technology, Shizuoka University, 3-5-1 Johoku, Hamamatsu 432-8011, Japan.
** Department of Electrical and Electronic Engineering, Shizuoka University, 3-5-1 Johoku, Hamamatsu 432-8561, Japan.

* Kinetic models are considering the motion of individual particles in the plasma sheath.

the scattering of the charged particles. The latter effect dominates at a pressure lower than 1 Torr where the orbital motion limit is satisfied. This result is contradictory with that of Chou, Talbot and Willis[12]. The collisional probe theory at the pressure higher than 100 Torr and for the plasma density higher than 10^{19} m^{-3} has not yet been so well developed as the collisionless probe theory. Very few collisional probe theories[15, 17] at such a high pressure and for high plasma density are available. In the continuum limit[15, 17], the mean free path of ions is much smaller than the Debye length, which is much smaller than R_p. Su and Lam[15] considered that the neutral particle density is sufficiently high so that both ions and electrons make numerous collisions with the neutral particles before being collected by the probe. Under their investigated discharge conditions, they found that at highly negative probe potentials the sheath thickness becomes comparable with R_p. They calculated numerically the probe characteristics for different probe sizes. Cohen[17] used the same theoretical model as proposed by Su and Lam, but he assumed that the probe potential V_p is less than or equal to the space potential ϕ. Cohen represented his results only in a graphical form, which is not convenient to use directly for the determination of plasma parameters. In the present paper, we have developed a technique which can provide plasma parameters directly for any D_λ from 50 to 1600 using Cohen's results.

2. Langmuir probe theory for high pressure plasma

In the present section the probe theory for the high pressure plasma will be reviewed. When the mean free paths are much smaller than R_P, the motion of the particles can be described by the collision dominated processes of diffusion and drift. Analysis of the probe characteristics is carried out by Cohen based on simultaneous solutions of Poisson's equation and continuity equations, in the case of $V_p < \phi$. The continuity equations for electrons and ions are given by

$$\vec{\nabla} \cdot \Gamma_e = -\frac{\partial N_e}{\partial t} = 0 \qquad (1)$$

$$\vec{\nabla} \cdot \Gamma_+ = -\frac{\partial N_+}{\partial t} = 0 \qquad (2)$$

where $N_{e,+}$ and $\Gamma_{e,+}$ are the densities and fluxes of electrons and ions, respectively. The flux equations for electrons and ions are given by

$$\vec{\Gamma}_e = -D_e \vec{\nabla} N_e + \mu_e N_e \vec{\nabla} \phi \qquad (3)$$

$$\vec{\Gamma}_+ = -D_+ \vec{\nabla} N_+ - \mu_+ N_+ \vec{\nabla} \phi \qquad (4)$$

where $D_{e,+}$ and $\mu_{e,+}$ represent the diffusion coefficients and mobilities of electrons and ions, respectively. Only electropositive plasmas are considered; i.e., electrons carry the entire negative charges. In such a case, no negative ion density or flux is considered and the Poisson's equation is given by

$$\nabla^2 \phi = -\frac{e}{\varepsilon_o}(N_+ - N_e) \qquad (5)$$

where ε_o and e are the permitivity of free space and the electronic charge, respectively.

The data of gas discharges are available in the literature by S. C. Brown[20], which allows one to determine $\mu_{e,+}$ as a function of electron or ion temperature $T_{e,+}$. To determine the diffusion coefficients the Einstein's relations for the electrons and ions are taken into account, i.e.,

$$D_{e,+} = \frac{\kappa T_{e,+}}{e} \mu_{e,+} \,, \qquad (6)$$

where κ is the Boltzmann constant.

Su and Lam considered a spherical probe in high density high pressure plasmas in the case where the probe is biased with a highly negative potential ϕ. In this case the electrons are in thermal equilibrium and their energies are in accord with the Boltzmann distribution. Furthermore they considered the case where λ_D is small compared with R_p and T_+/T_e is also small. They found that for small λ_D, the quasi-neutral solution breaks down near the probe surface and an ion sheath is formed in front of the probe. In order to satisfy the condition of $N_e=N_+=0$ at the probe surface, a very thin ion diffusion layer should appear within the ion sheath when T_+/T_e is small. However, Cohen assumed that the plasma density is sufficiently high and that ions and electrons make many collisions with the neutral particles before being collected by the probe. He concentrated the analysis of the probe characteristics to the case of $V_p \le \phi$. Cohen solved the above macroscopic particle flux equations by applying Einstein's relation together with the Maxwell's equation and Poisson's equation in the asymptotic limits of $D_\lambda \to \infty$, $T_+/T_e \to 0$ and $0 \le \varphi_p \le \ln(D_\lambda)$ in order to determine the spatial profiles of plasma density and space potential, where φ_p is defined by

$$\varphi_p = -\frac{e(V_p - \phi)}{\kappa T_e}. \qquad (7)$$

Cohen assumed that $D_{e,+}$, $\mu_{e,+}$ and $T_{e,+}$ are constant over the space. He also assumed that the mean free paths of electrons and ions λ_e and λ_+ are smaller than the sheath size.

The one-dimensional solutions[15] of the continuity equations and the Poisson's equation for the spherical probe at $\varphi_p = 0$ are given by

$$N_e(r) = N_o\left(1 - \frac{I_e}{4\pi N_o e D_e}\frac{1}{r}\right) \qquad (8a)$$

$$N_+(r) = N_o\left(1 - \frac{I_+}{4\pi N_o e D_+}\frac{1}{r}\right) \qquad (8b)$$

where N_o is N_e and N_+ at $r = \infty$, *i.e.*, $N_e(\infty)=N_+(\infty)=N_o$.

In Eq. (8a), the electron current I_e collected by the probe at $\varphi_p = 0$ should be equal to the random electron current I_{eR}. It is reasonable to assume that $N_+=N_e=0$ at the probe surface. Therefore I_{eR} can be derived from Eq. (8a) as follows,

$$I_{eR} = 4\pi R_p e N_o D_e \qquad (9)$$

with

$$D_e = \frac{1}{3}\lambda_e v_{e,th} \qquad (10)$$

$$\lambda_e = \frac{1}{N_o \sigma_{c,e}} \qquad (11)$$

$$v_{e,th} = \sqrt{\frac{8\kappa T_e}{\pi m_e}} \qquad (12)$$

where $v_{e,th}$, m_e and $\sigma_{c,e}$ are the thermal velocity, mass and total collision cross section of electrons, respectively. The random electron flux per unit probe surface area, Γ_{eR} can be written as

$$\Gamma_{eR} = \frac{I_{eR}}{4\pi R_p^2 e} = \frac{N_o v_{e,th}}{4}\left(\frac{4}{3}\frac{\lambda_e}{R_p}\right). \quad (13)$$

It should be noted that Γ_{eR} is reduced by a factor of $4\lambda_e/3R_p$ compared with the case where collisions are absent in the sheath region.

Numerical results calculated by Cohen give the relations between I_e or I_+ and V_p in the graphical forms for the selected values of D_λ taken as a parameter. It should be noted that the analytical formulae for the probe characteristics are not available in Cohen's analysis. However, for the determination of plasma parameters from the measured probe characteristics, the modeling of the probe characteristics for an arbitrary D_λ is required. In the present paper, we have developed a method which provides a set of algebraic formulae by fitting the assumed functions such as the Gaussian or Boltzmann function to the graphically presented results by Cohen. From Eq. (13), I_{eR} is rewritten by

$$I_{eR} = eS\Gamma_{eR} = \frac{4}{3}\pi R_p e N_o \lambda_e v_{e,th} \quad (14)$$

where $S=4\pi R_p^2$ is the surface area of the spherical probe. The value of I_e for an arbitrary φ_p can be presumably expressed by introducing a function $I_{en}(\varphi_p, D_\lambda)$ as follows

$$I_e = I_{eR} I_{en}(\varphi_p, D_\lambda). \quad (15)$$

Most of the present work was devoted to determining $I_{en}(\varphi_p, D_\lambda)$ using the numerical results by Cohen. The probe current I_p consists of I_+, I_e and the current I_{em} which is caused by the secondary electrons emitted from the probe surface. In the high pressure high density plasmas, a large amount of secondary electrons can be emitted from the probe surface due to the Auger neutralization of ions or the Auger de-excitation of metastable excited atoms at the probe surface. In such a case, I_p is given by

$$I_p = I_e - I_+ - I_{em}. \quad (16)$$

With decreasing pressure, the contribution of I_{em} to I_p decreases due to increasing wall losses of metastable excited atoms. For the pressure lower than 100 Torr, I_+ is already much higher than I_{em} so that Eq. (16) reduces to

$$I_p = I_e - I_+. \quad (17)$$

In this case, $N_+(\infty)$ can be determined independently from $N_e(\infty)$ using the ion branch of the probe characteristics. For this purpose, an expression for I_+ is needed. Again the results of Cohen's analysis can be applied. The useful expressions to estimate $N_+(\infty)$ can be derived by the same procedure as that for electrons,

$$I_{+R} = 4\pi N_o e D_+ R_P = \frac{4}{3}\pi R_p e N_o \lambda_+ v_{+,th} \quad (18)$$

$$\Gamma_{+R} = \frac{I_{+R}}{4\pi R_p^2 e} = \frac{N_o v_{+,th}}{4}\left(\frac{4}{3}\frac{\lambda_+}{R_p}\right) \quad (19)$$

with

$$D_+ = \frac{1}{3}\lambda_+ v_{+,th} \quad (20)$$

$$\lambda_+ = \frac{1}{N_o \sigma_{c,+}} \quad (21)$$

$$v_{+,th} = \sqrt{\frac{8\kappa T_+}{\pi m_+}} \quad (22)$$

where I_{+R} and Γ_{+R} are the ion random current to the probe and the ion flux per unit probe surface area and m_+, $\sigma_{c,+}$ and $v_{+,th}$ are the mass, collision cross section and thermal velocity of ions, respectively. Again Γ_{+R} is reduced by a factor of $4\lambda_+/3R_p$ as compared with the case where there is no collision in the sheath region.

The ion current I_+ for an arbitrary φ_p is presumed as

$$I_+ = I_{+R}\left(\frac{T_+}{T_e}\right) I_{+n}(\varphi_p, D_\lambda) \quad (23)$$

where $I_{+n}(\varphi_p, D_\lambda)$ is a function which should be determined based on Cohen's analysis.

3. Algebraic equations derived for electron and ion current to the probe using Cohen's analysis

Relations between I_{en} or I_{+n} and φ_p numerically calculated by Cohen under conditions of $T_+/T_e \rightarrow 0$ for several D_λ are available as shown by the marks in Figs. 1(a) and 2(a). In the present work an algebraic equation $I_{en}(\varphi_p, D_\lambda)$ best fitted to Cohen's results is deduced by modifying Gaussian function. After somewhat tedious considerations concerned with the dependence of I_{en} on φ_p, $I_{en}(\varphi_p, D_\lambda)$ is empirically presumed as follows:

$$I_{en} = \frac{13.314}{n}\exp\left\{-2\left(\frac{\varphi_p - m}{n}\right)^2\right\}. \quad (24)$$

Figure 1(a) shows that the solid curves calculated by Eq. (24) fit well with Cohen's data for each D_λ, by adjusting the values of m and n. Table 1 summarizes the dependence of m and n on D_λ. However, at this moment, the values of m and n can be applied only for six values of D_λ used for fitting. In the practical use, m and n should be given as a function of D_λ. Fortunately m and n can be approximated by polynomial and logarithmic functions of D_λ, respectively, as follows:

$$m(D_\lambda) = -4.154 + 2.429\times 10^{-4} D_\lambda - 5.023\times 10^{-8} D_\lambda^2, \quad (25)$$

and

$$n(D_\lambda) = 6.044 + 0.55\log(D_\lambda), \quad (26)$$

For reference, the fitted curves of $m(D_\lambda)$ and $n(D_\lambda)$ are shown in **Fig. 1(b)**. Using Eq. (24) along with Eqs. (25) and (26), one can easily fit $I_{en}(\varphi_p, D_\lambda)$ to any D_λ from 50 to 1600.

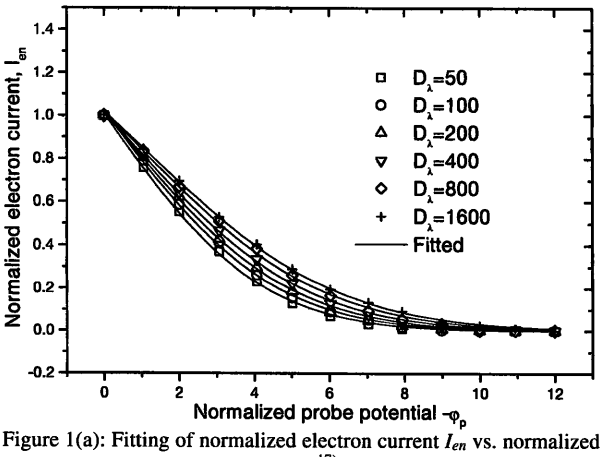

Figure 1(a): Fitting of normalized electron current I_{en} vs. normalized probe potential φ_p (data[17] have been collected from Fig. 4).

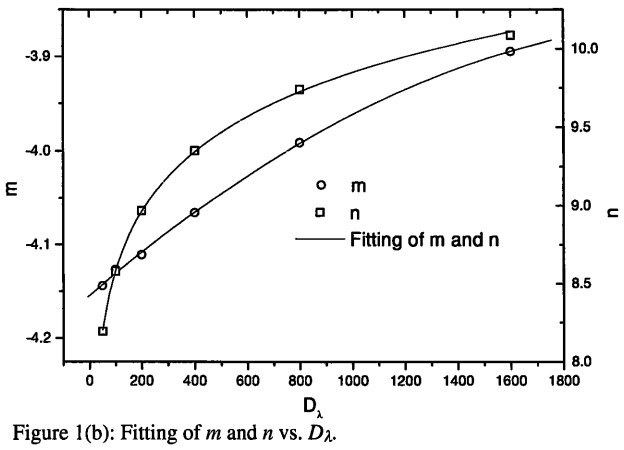

Figure 1(b): Fitting of m and n vs. D_λ.

Table1: Dependence of m and n on D_λ.

D_λ	m	n
50	8.19433	-4.14385
100	8.5805	-4.1265
200	8.9684	-4.11063
400	9.35344	-4.06581
800	9.74051	-3.99136
1600	10.08626	-3.89445

The secondary electron emission current[18] I_{em} is given by

$$I_{em} = \frac{eN_m v_m S\gamma_m}{4}, \tag{27}$$

where N_m is the density of metastable atoms, v_m is the average velocity of the metastable atoms and γ_m is the secondary electron emission coefficient. For the high pressure, I_{em} is much higher than I_+. Disregarding I_+ with respect to I_{em}, Eq. (16) can be written as

$$I_p = I_{eR} I_{en}(\varphi_p, D_\lambda) - I_{em}, \tag{28}$$

which can be treated as the electron saturation current*. Now, one can easily apply Eq. (28) along with Eq. (24) to analyze the probe characteristics measured in the high pressure plasmas.

As for $I_{+n}(\varphi_p, D_\lambda)$, its dependence on φ_p given by Cohen's numerical results suggests the next fitting function based on the modified Boltzmann function

$$I_{+n} = \frac{T_e}{T_+}\left\{A_2 + \frac{A_1 - A_2}{1+\exp\left(\frac{\varphi_p - p}{2.50}\right)}\right\}. \tag{29}$$

As in the case of $I_{en}(\varphi_p, D_\lambda)$, A_1, A_2 and p are obtained in such a way that I_{+n} -φ_p curves are best fitted to the Cohen's numerical results which are summarized for six values of D_λ in Table 2. **Figure 2(b)** shows the curves best fitted to A_1, A_2 and p. The curves are expressed by rational functions for A_1 and A_2 and a sigmoidal logistic function for p, respectively as

$$A_1(D_\lambda) = \frac{-1.252 - 0.002D_\lambda}{1+0.0042D_\lambda}, \tag{30}$$

$$A_2(D_\lambda) = \frac{1.774 + 0.038D_\lambda}{1+0.036D_\lambda}, \tag{31}$$

and

$$p(D_\lambda) = \frac{1.672}{1+3.345\exp(-0.0037D_\lambda)}. \tag{32}$$

Using Eq. (29) along with Eqs. (30), (31) and (32), one can fit $I_{+n}(\varphi_p, D_\lambda)$ for any D_λ from 50 to 1600. Now, utilizing Eq. (23) together with Eq. (29) under the mentioned conditions, one can analyze the probe characteristics obtained in the high pressure plasmas. The expression of Cohen's results by using simple algebraic functions allows one to use iterative procedures in the next section for the determination of plasma parameters and to avoid making the fitting parameters discrete.

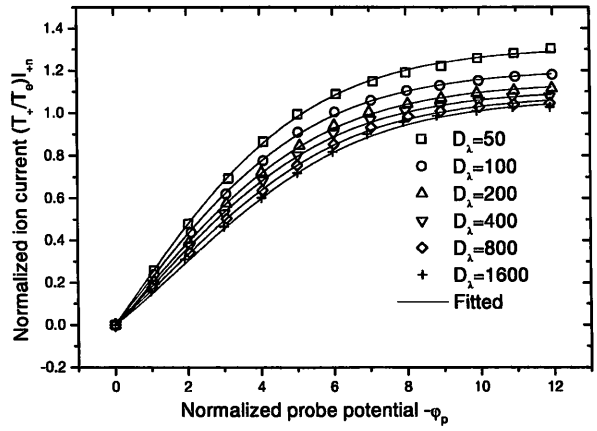

Figure 2(a): Fitting of normalized ion current I_{+n} vs. normalized probe potential φ_p (data[17] have been collected from Fig. 4).

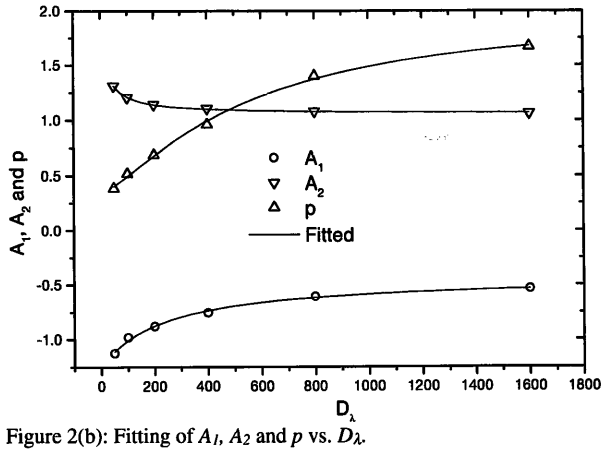

Figure 2(b): Fitting of A_1, A_2 and p vs. D_λ.

Table2: Dependence of A_1, A_2 and p on D_λ.

D_λ	A_1	A_2	p
50	1.12501	1.31191	0.38486
100	0.98238	1.20603	0.51786
200	0.8797	1.14344	0.6869
400	0.75678	1.108	0.96113
800	0.60697	1.0792	1.40106
1600	0.5349	1.06233	1.67109

4. Probe characteristic measurement in high pressure microwave discharges

The probe characteristics are measured in the high pressure microwave discharge. **Figures 3(a)** and **3(b)** show the schematic diagrams of the experimental setup developed to produce non-equilibrium plasmas and the cross sectional view of a discharge chamber. The detailed description of the setup was published elsewhere[1]. The discharge chamber is made of a rectangular waveguide 54 mm high, 108 mm wide and 130 mm long. Open ends of the rectangular waveguide are closed by pyrex glass plates in order to form the discharge chamber. Two cylindrical pipes made of tungsten, 4 and 6 mm in inner and outer diameters, respectively, are inserted perpendicularly through the wider walls of the rectangular waveguide, as shown in **Fig. 3(b)**. The spacing between the stub tips is maintained at 10 mm. In order to make a Langmuir probe, a tungsten wire of 0.8mm in diameter embedded in the insulation of an alumina tube, is inserted through one of the stubs as shown in **Fig. 3(b)**. The probe tip 1 mm long is placed at the center of the stub and along its axis. A 1.5kW at the maximum, 2.45GHz pulsed magnetron with a repetition frequency of 120Hz is used as a microwave power source. Helium is used as working gas.

Figure 4 shows the probe characteristics measured at the helium pressures of 100, 300 and 700 Torr. It is found that I_p measured at 700 Torr has a dip around V_p from 0 to -40V. The dip is caused by I_{em}, which is induced by the excited helium atoms. On the other hand, for 100 and 300 Torr, the probe characteristics do not exhibit the remarkable secondary emission from the probe. It seems that the production rate of metastable excited helium atoms grows almost proportional to the helium pressure. Thus I_{em} becomes predominant at 700 Torr.

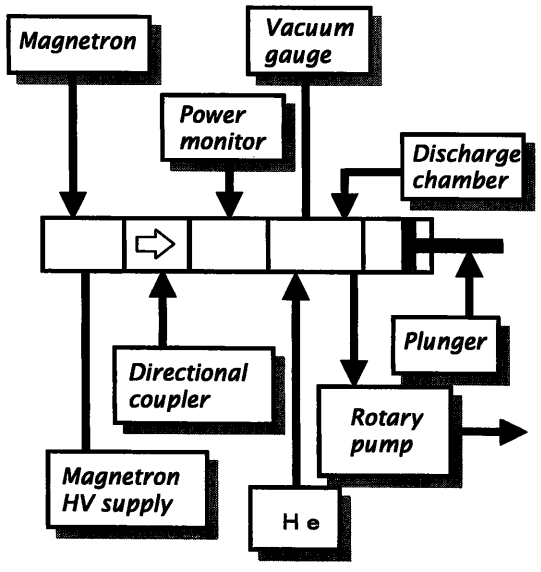

Figure 3(a): Schematic diagram of the experimental setup.

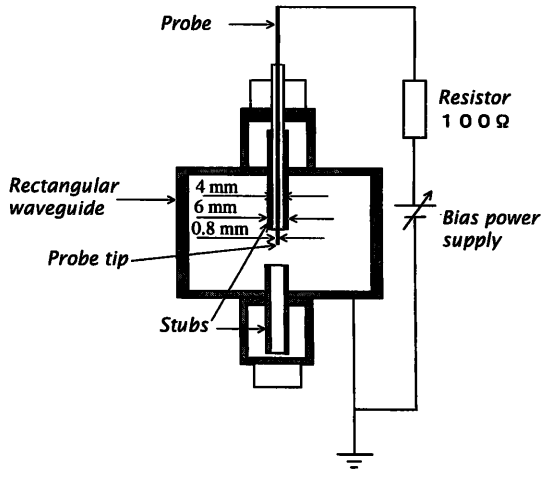

Figure 3(b): Cross-sectional view of the discharge chamber.

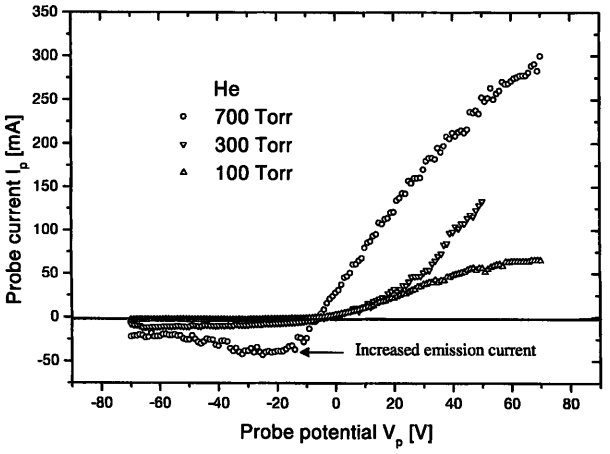

Figure 4: Current-voltage probe characteristics at 80 μ sec after the starting of the microwave power pulse. A tungsten probe is used.

Table 3: Variation of plasma parameters with pressure. Data considered only at 80 μ sec after the onset of the discharge for 100, 300 and 700 Torr, respectively.

Pressure P (Torr)	Electron density N_e (m^{-3})	Debye length λ_D (m)	Debye number $D\lambda$	Electron temperature T_e (eV)	Space potential ϕ (V)
100	1.50×10^{19}	4.30×10^{-6}	114	5	30
300	1.36×10^{20}	1.38×10^{-6}	355	4.69	27
700	5.36×10^{20}	6.82×10^{-7}	718	5	16

5. Analysis of measured probe characteristics

To obtain the plasma parameters, probe characteristics measured in high pressure microwave discharges have been fitted using an iterative procedure shown by a flow chart in **Fig 5**. The best-fitted curve can provide T_e, N_e, I_{em} and ϕ. At first, the probe characteristic obtained at 700 Torr of helium shown in **Fig. 6** is introduced for the estimation of plasma parameters. We have selected a portion from the whole probe characteristic for fitting as shown in **Fig. 6**. The part of the probe characteristic to be fitted has been selected in the following way. The point where the probe characteristic just starts bending gives the upper limit of the curve, as shown by a point B in **Fig. 6**. The lower limit of

* The term "electron saturation current" is used in analogous to the probe characteristics in collisionless case. It is not the "electron saturation current" in the sense of thermal flux in the plasma bulk.

the curve is chosen as the minimum probe current in the probe characteristic, as shown by a point *A* in **Fig. 6**. In the estimation this minimum current is treated as I_{em}. For the increase of I_{em} under a pressure higher than 100 Torr, the ion part of the probe characteristic should not be used otherwise it could provide over-estimation of N_+. The proposed fitting technique takes I_{em} into account, and allows one to obtain reasonable plasma parameters even for very strongly distorted probe characteristics in the case of the atmospheric pressure.

The probe current I_p has been fitted using Eq. (28). The final value of N_e is calculated using the following equation

$$N_e = \frac{I_{eR,n} + I_{em,n}}{4\pi R_p e D_{e,n}} \tag{33}$$

where $I_{eR,n}$, $I_{em,n}$ and $D_{e,n}$ are the calculated electron saturation current, the secondary electron emission current and the diffusion coefficient at the *n-th* iteration, respectively. The relative error used for the evaluation of fitting is formulated as the probe current, and thus the relative error ε_i is given by

$$\varepsilon_{i+1} = \sqrt{\frac{\sum_{j=0}^{k}\left(\frac{I_{M,j} - I_{C,i,j}}{I_{M,j}}\right)^2}{k}} \tag{34}$$

where $i=1,2,3....n$ is the number of iterations; $j=1,2,3....k$ is the number of measured points; $I_{M,j}$ is the measured probe current at the *j-th* point and $I_{C,i,j}$ is the calculated probe current in the *i-th* iteration and at the *j-th* point, respectively. The iteration procedure shown in **Fig. 5** for the determination of plasma parameters is described below.

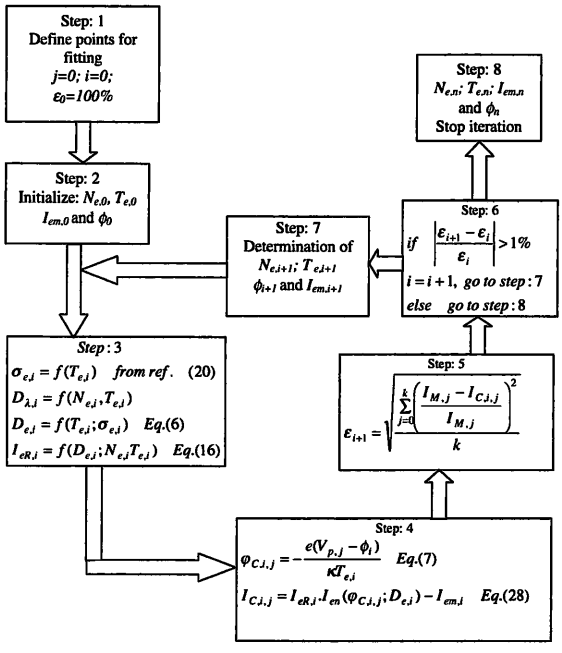

Figure 5: Flow chart for the determination of plasma parameters.

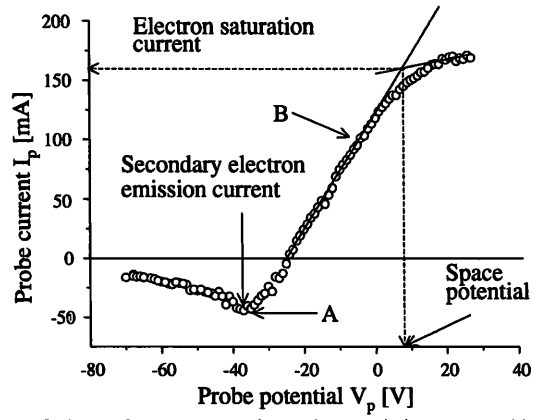

Figure 6: Anomalous current-voltage characteristics measured by the tungsten probe at the helium pressure of 700 Torr.

Step 1: One has to define the parameters: (a) The number of data points *j* to be considered. This will specify a portion from the whole probe characteristic, which is to be considered for fitting. (b) The number of iterations *i* can be initialized by *0*. (c) The estimated error ε_0 can be initialized as 100%.

Step 2: The values of N_e, T_e, I_{em} and ϕ can be initialized by assumption. If these initialized values are very close to the calculated ones, even a few iterations can provide the best fitting. Otherwise, the number of iterations will be increased to get the best fitting.

Step 3: The value of σ_e can be found from the reference (20). The values of D_e and I_{eR} can be determined using Eqs. (6) and (14), respectively.

Step 4: The values of φ_p and I_p in the iteration process can be calculated by using Eqs. (7) and (28), respectively. These two equations can be written as

$$\varphi_{C,i,j} = -\frac{e(V_{p,j} - \phi_i)}{\kappa T_{e,i}}, \tag{35}$$

and

$$I_{C,i,j} = I_{eR,i}.I_{en}(\varphi_{C,i,j}; D_{e,i}) - I_{em,i} \tag{36}$$

where $\varphi_{C,i,j}$ is the calculated normalized probe potential at the *j-th* point and in the *i-th* iteration, $V_{p,j}$ is the probe potential at the *j-th* point, ϕ_i , $T_{e,i}$, $I_{eR,i}$, $D_{e,i}$ and $I_{em,i}$ are the space potential, the electron temperature, the random electron current, the electron diffusion coefficient and the secondary electron emission current in the *i-th* iteration, respectively.

Step 5: Relative error ε_i is estimated using Eq. (34).

Step 6: Compare ε_i and ε_{i+1}. If $|(\varepsilon_{i+1} - \varepsilon_i)/\varepsilon_i| > 1\%$, the next iteration will be started by taking the new values of N_e , T_e , I_{em} and ϕ .

Step 7: If $|(\varepsilon_{i+1} - \varepsilon_i)/\varepsilon_i| \le 1\%$, the iteration will be finished and the best-fitted curve will provide the plasma parameters N_e , T_e , I_{em} and ϕ . Examples of the best fitted curves are shown in Figs. 7(a), 7(b) and 7(c) for the pressures of 100, 300 and 700 Torr, respectively.

The ion current I_+ has been fitted for 100 Torr only, assuming T_+=1000K according to Eq. (23) by an analogous procedure as that of the electron current fitting. In this case, the values of T_e and ϕ are used, which were obtained from the electron current fitting. The value of N_+ can be calculated neglecting I_{em} and using the following equation

$$N_+ = \frac{3I_{+R,n}T_+}{4\pi R_p e \lambda_+ v_{+,th} T_e} \tag{37}$$

where $I_{+R,n}$ is the final value of I_{+R} obtained by the fitting.

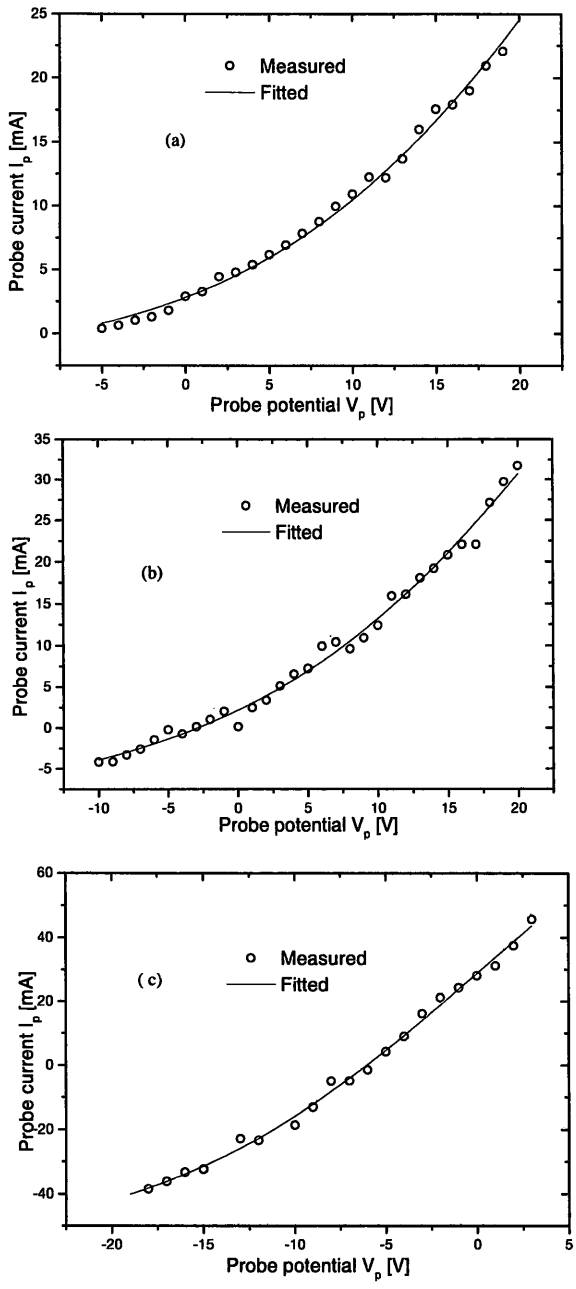

Figure 7: Fitting of the probe current I_p measured at 80 μ sec after the starting of the microwave power pulse: (a) 100 Torr, (b) 300 Torr and (c) 700 Torr.

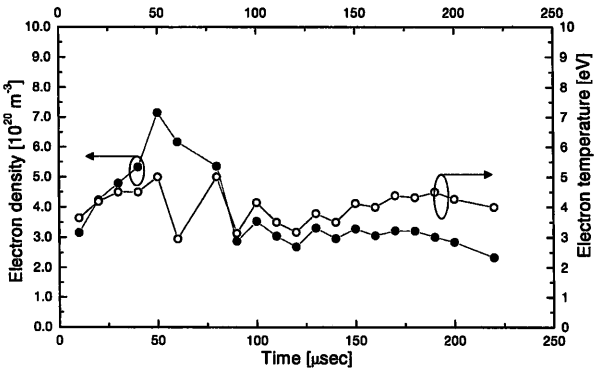

Figure 8: Temporal development of the electron density and temperature in a helium-discharge at 700 Torr after the starting of the microwave power pulse.

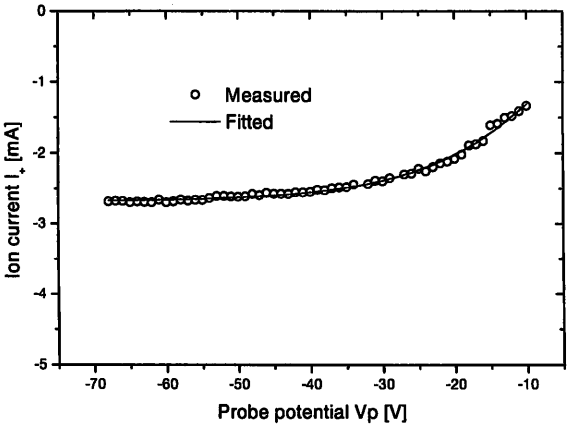

Figure 9: Comparison between the measured and fitted ion currents to the probe.

6. Estimation of plasma parameters and discussion

The plasma parameters estimated from the probe characteristics shown in **Figs.7(a)** through **7(c)** for several pressures are given in Table 3. It can be seen that N_e at 80 μ sec after the onset of the discharge increases with increasing P. On the other hand ϕ decreases with the increase of P.

Figure 8 shows the time evolution of T_e and N_e for 700 Torr. At the beginning of the discharge, T_e and N_e are lower and increase with increasing time, reaching the maximum at 50 μ sec. After 50 μ sec, they start decreasing, continuously decreasing up to 80 μ sec and then getting saturated.

For 100 Torr, the probe characteristics do not exhibit the strong influence of I_{em} on their shapes as shown in **Fig. 4**. The negative currents for the highly negative probe potential can be interpreted as ion currents I_+.

The ion saturation current has been fitted using Eq. (23) for 100 Torr at 80 μ sec after the onset of the discharge as shown in **Fig. 9**. The estimated value of N_+ is 1.67×10^{19} m^{-3}, while under the same condition, N_e is 1.50×10^{19} m^{-3} obtained by fitting the electron current using equation (28). Discrepancies of N_+ and N_e may be occurred by the following reasons: the values of T_+ and T_g used in the estimation are different from that of Cohen's model, i.e., (1) T_+ = 1000 K; as can be seen from Eq. (37) that N_+ can be changed depending on T_+ so that the assumed T_+ = 1000 K may not be true. (2) Gas temperature T_g = 300 K; which may be different in the experiment because of the dependence of λ_+ on T_g. (3) The fitting procedure can also provide error. Moreover, those densities obtained by the probe measurement are considered to have an error around few percent. Above all, it is seen that N_e and N_+ are providing a good agreement.

7. Conclusion

High pressure helium microwave discharge by the moderate microwave power of 400W has been investigated by a Langmuir probe. A method for the determination of T_e, N_e and N_+ is established. Simple algebraic functions allow one to use iterative procedures for the determination of plasma parameters and avoid making the fitting parameters discrete. The proposed fitting technique takes into account

the secondary electron emission current, and allows one to obtain reasonable plasma parameters even for much distorted probe characteristics.

References

1) M. Kando, 11th Symposium on elementary processes and chemical reactions in low temperature plasma, Low Tatras, Slovakia, **June**, 73 (1998).

2) O.A. Ivanov, A.M. Gorbachev, V.A. Koldanov, A.L. Kolisko and A.L. Vikharev, J. Phys. IV France **8**, 317 (1998).

3) J. Park, I. Henins, H.W. Herrmann, G.S. Selwyn, J.Y. Jeong, R.F. Hicks, D. Shim and C.S. Chang, Appl. Phys. Lett. **76**, 288 (2000).

4) H. Takeyama, "High pressure microwave discharge", report submitted for the graduation of the Masters course at the M. Kando Lab., Shizuoka University, 1998.

5) H.M. Mott-Smith and I. Langmuir, Phys. Rev. **28**, 727 (1926).

6) J.F. Waymouth, Phys. Fluids **7**, 1843 (1964).

7) G.K. Bienkowski and K.W. Chang, Phys. Fluids **11**, 784 (1968).

8) E. Wasserstrom, C.H. Su, and R.F. Probstein, Phys. Fluids **8**, 56 (1965).

9) Z. Zakrzewski and T. Kopiczynski, Plasma Phys. **16**, 1195 (1974).

10) A. K. Jakubowski, AIAA Journal **10**, 988 (1972).

11) G. J. Schulz and S. C. Brown, Phys. Rev. **98**, 1642 (1955).

12) Y.S. Chou, L. Talbot and D.R. Willis, Phys. Fluids **9**, 2150 (1966).

13) M. Tichy, M. Sicha, P. David and T. David, Contrib. Plasma Phys **34**, 59 (1994).

14) M. Sicha, M. Tichy, V. Hrachova, P. David, T. David and J. Tous, Contrib. Plasma Phys **34**, 51 (1994).

15) C.H. Su and S.H. Lam, Phys. Fluids **6**, 1479 (1963).

16) R.E. Kiel, Phys. Fluids **40**, 3668 (1969).

17) I. M. Cohen, Phys. Fluids **6**, 1492 (1963).

18) Yu. M. Kagan and V. I. Perel, Soviet Phys., Uspekhi May-June, 767 (1964).

19) F.F. Chen, Plasma Diagnostic Technique, Edited by Huddleston and Leonard, Academic Press, New York, 1965.

20) S.C. Brown, Basic Data of Plasma Physics, second edition, The MIT Press (1964).